

Long range statistical fluctuations of the crossed Josephson current

Régis Mélin*

*Centre de Recherches sur les Très Basses Températures (CRTBT[†]),
CNRS, BP 166, 38042 Grenoble Cedex 9, France*

We investigate the crossed Josephson effect in a geometry consisting of a double ferromagnetic bridge between two superconductors, with tunnel interfaces. The crossed Josephson current vanishes on average because the Andreev reflected hole does not follow the same sequence of impurities as the incoming electron. We show that i) the root mean square of the crossed Josephson current distribution is proportional to the square root of the junction area; and ii) the coherent coupling mediated by fluctuations is “long range” since it decays over the ferromagnet phase coherence length l_φ , larger than the exchange length. We predict a crossed Josephson current due to fluctuations if the length of the ferromagnets is smaller than l_φ and larger than the exchange length ξ_h .

PACS numbers: 74.50.+r,74.78.Na,74.78.Fk

I. INTRODUCTION

Transport properties of hybrid structures consisting of a superconductor (S) multiply connected to several normal metal (N) or ferromagnetic (F) electrodes has focused an important interest recently^{1,2,3}. In usual Andreev reflection at a single NS interface, a spin-up electron coming from the N side is reflected as a hole in the spin-down band while a Cooper pair is transferred in the superconductor. Multiterminal structures allow “non local” processes, in which a spin-up electron in one electrode is Andreev reflected as a hole in the spin-down band in another electrode, corresponding to non local transmission in the electron-hole channel. Conversely non local transmission in the electron-electron channel corresponds to a process in which a spin-up electron from one electrode is transmitted as a spin-up electron in another electrode. Transport theory of three-terminal FSF junctions including non local transmission in the electron-electron and electron-hole channels has been discussed recently^{4,5,6,7,8,9,10,11,12,13,14,15,16,17,18}, in the tunnel limit^{4,5} and for highly transparent interfaces^{6,7}, on the basis of microscopic Green’s functions^{4,6,7,8,9,10} and in the framework of the scattering approach^{11,12,13}. The models were also extended to describe disorder^{14,15,16}, non collinear ferromagnets⁹, and the noise^{17,18}. On the experimental side, two experiments probing non local transport were carried out recently^{19,20}, in FSF and NSN three-terminal junctions.

The question arises of whether the phase coherence of crossed Andreev reflection can be probed experimentally. We show here that this is possible with a double ferromagnetic bridge between two superconductors (see Fig. 1). We have already shown that the crossed Josephson current vanishes on average in the diffusive limit⁹, because the Andreev reflected hole does not follow the same sequence of impurities as the incoming electron since they propagate in different electrodes. However, by evaluating the statistical fluctuations of the dc crossed Josephson current, we show here that the fluctuations of the Josephson current decay over the phase coherence length l_φ in the ferromagnet, larger than the decay length of the local average Josephson current set by the exchange length ξ_h (see Refs. 21,22,23,24,25,26,27,28,29,30). The fluctuations of the crossed supercurrent do not show π -shift oscillations and damping as a function of the ferromagnet length, because the spin-up and spin-down electrons of correlated pairs extracted from one superconductor do not see the same realization of disorder, so that the center of mass momentum of the spatially separated correlated pair averages to zero after propagation over a length comparable to the elastic mean free path. The root mean square of the crossed Josephson current is proportional to the square root of the junction area, because the number of diagrams involved in the supercurrent is equal to the junction area divided by the Fermi wave-length. The crossed Josephson supercurrent due to fluctuations can in principle be detected experimentally, provided the length of the ferromagnets is smaller than l_φ and larger than ξ_h .

The article is organized as follows. Preliminaries regarding Green’s functions are given in section II. The analytical results are presented in section III for the average local supercurrent, and in section IV for the statistical fluctuations of the supercurrent. Concluding remarks are given in section V. Some details on disorder averaging are provided in the Appendix.

* regis.melin@grenoble.cnrs.fr

† U.P.R. 5001 du CNRS, Laboratoire conventionné avec l’Université Joseph Fourier

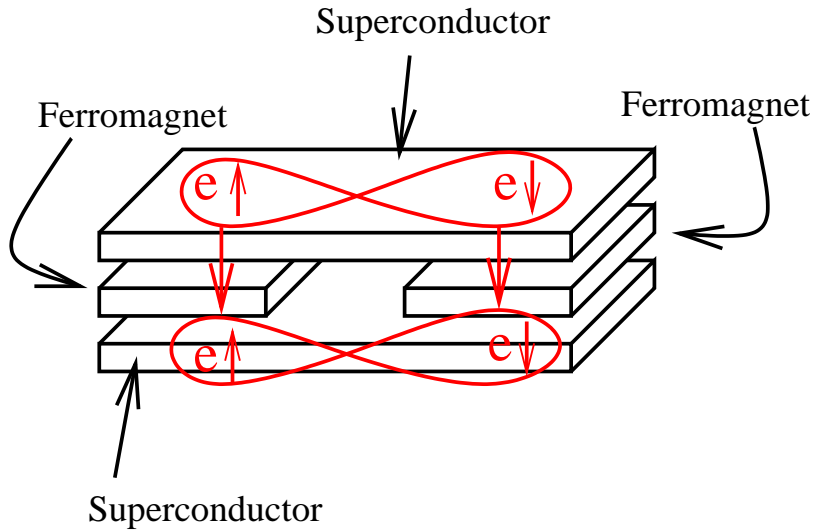


FIG. 1: (Color online.) Schematic 3D representation of the Josephson junction considered in the article.

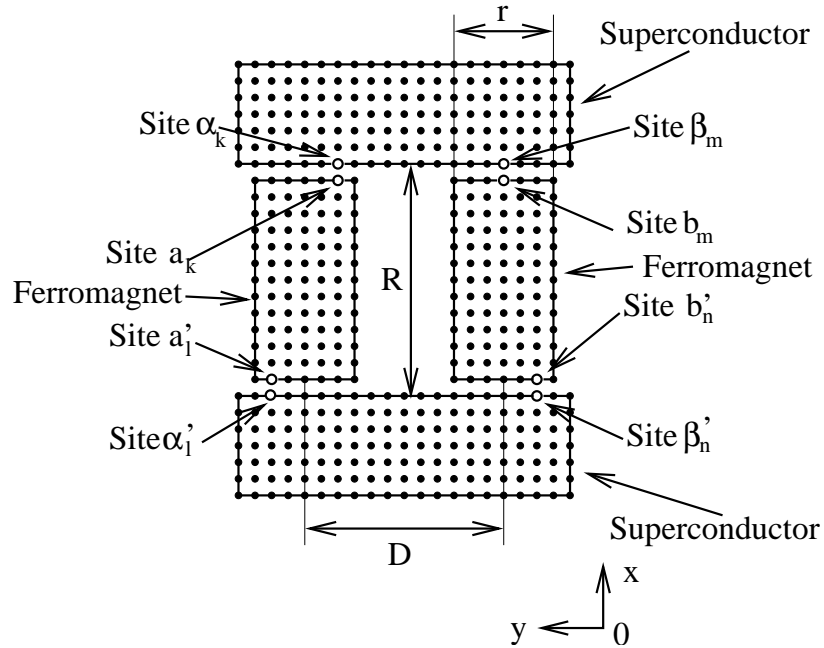


FIG. 2: Schematic 2D cut of the junction on Fig. 1. We have represented some pairs of sites at the interfaces: (a_k, α_k) , (a'_l, α'_l) , (b_m, β_m) , and (b'_n, β'_n) .

II. TECHNICAL PRELIMINARIES

A. The models

The superconductor is described by the BCS Hamiltonian

$$\mathcal{H}_{\text{BCS}} = \sum_{(\alpha, \beta), \sigma} -t \left(c_{\alpha, \sigma}^{\dagger} c_{\beta, \sigma} + c_{\beta, \sigma}^{\dagger} c_{\alpha, \sigma} \right) + \Delta \sum_{\alpha} \left(c_{\alpha, \uparrow}^{\dagger} c_{\alpha, \downarrow}^{\dagger} + c_{\alpha, \downarrow} c_{\alpha, \uparrow} \right), \quad (1)$$

where t is the hopping amplitude, Δ is the superconducting gap, and α and β correspond to neighboring sites on a cubic lattice with a parameter a_0 . The lattice parameter a_0 is taken equal to the Fermi wave-length λ_F . The

ferromagnetic electrodes are described by the Stoner model

$$\mathcal{H}_{\text{Stoner}} = \sum_{\langle\alpha,\beta\rangle,\sigma} -t \left(c_{\alpha,\sigma}^+ c_{\beta,\sigma} + c_{\beta,\sigma}^+ c_{\alpha,\sigma} \right) - h_{\text{ex}} \sum_{\alpha} \left(c_{\alpha,\uparrow}^+ c_{\alpha,\uparrow} - c_{\alpha,\downarrow}^+ c_{\alpha,\downarrow} \right), \quad (2)$$

where h_{ex} is the exchange field. The exchange fields in the two ferromagnets are equal in the parallel alignment, and opposite in the antiparallel alignment. We incorporate also disorder scattering, described by the Hamiltonian

$$\mathcal{H}_{\text{dis}} = \sum_{\alpha_n,\sigma} V_{\alpha_n} c_{\alpha_n,\sigma}^+ c_{\alpha_n,\sigma}, \quad (3)$$

where the impurities are located at the sites α_n . The impurity scattering potentials V_{α_n} are random variables. The site a_k is on the ferromagnetic side of the interface, and the site α_k on the superconducting side.

The couplings between the ferromagnets and the superconductors are described by the tunnel Hamiltonian. The tunnel Hamiltonian at the interface (a, α) takes the form

$$\mathcal{W}_{a,\alpha} = \sum_{k,\sigma} \left(-t_{a_k,\alpha_k} c_{a_k,\sigma,F}^+ c_{\alpha_k,\sigma,S} - t_{\alpha_k,a_k} c_{\alpha_k,\sigma,S}^+ c_{a_k,\sigma,F} \right), \quad (4)$$

where the summation runs over all sites at the interface (see Fig. 2), and where $t_{a_k,\alpha_k} = t_{\alpha_k,a_k}$ is the hopping amplitude connecting the sites a_k and α_k .

B. Green's functions of a ferromagnet and a superconductor

The starting point is the ballistic Green's function $\hat{g}_{i,j}(\omega)$ of the isolated ferromagnetic and superconducting electrodes in the Nambu representation. The ballistic Green's functions of a ferromagnet take the form

$$g_{a,b}^{\uparrow,1,A}(\omega) = -\frac{\pi\rho_F}{k_F d_{a,b}} \exp \left[-i \left(k_F^{\uparrow} + \frac{\omega}{\hbar v_F^{\uparrow}} \right) d_{a,b} \right] \exp(-d_{a,b}/l_{\varphi}^{(\text{ball})}) \quad (5)$$

$$g_{a,b}^{\uparrow,2,A}(\omega) = \frac{\pi\rho_F}{k_F d_{a,b}} \exp \left[i \left(k_F^{\downarrow} - \frac{\omega}{\hbar v_F^{\downarrow}} \right) d_{a,b} \right] \exp(-d_{a,b}/l_{\varphi}^{(\text{ball})}), \quad (6)$$

where $g_{a,b}^{\uparrow,1}$ and $g_{a,b}^{\uparrow,2}$ are the Green's functions of a spin-up electron and a hole in the spin-down band respectively, both having $S_z = 1/2$, $d_{a,b}$ is the distance between the sites a and b , ω the energy with respect to the chemical potential, ρ_F the density of states, k_F^{\uparrow} and k_F^{\downarrow} the spin-up and spin-down Fermi wave-vectors, v_F^{\uparrow} and v_F^{\downarrow} the spin-up and spin-down Fermi velocities. The ballistic ferromagnet Green's functions given by Eqs. (5) and (6) decay exponentially over the phase coherence length $l_{\varphi}^{(\text{ball})}$, introduced phenomenologically through an imaginary part $\hbar v_F/l_{\varphi}^{(\text{ball})}$ to the energy ω . We note k_F and v_F the Fermi wave-vector and the Fermi velocity in the absence of spin polarization. We neglect in the following the energy dependence of the ferromagnet propagators in Eqs. (5) and (6) since we suppose that the length R of the ferromagnets is small compared $\hbar v_F^{\uparrow}/\Delta$ and $\hbar v_F^{\downarrow}/\Delta$, both length scales being comparable to the ballistic BCS coherence length $\hbar v_F/\Delta$.

The Nambu Green's function of a ballistic isolated superconductor in the sector $S_z = 1/2$ takes the form

$$\hat{g}_{\alpha,\beta}(\omega) = \frac{\pi\rho_S}{k_F d_{\alpha,\beta}} \exp \left(-\frac{d_{\alpha,\beta}}{\xi_{\text{BCS}}^{(\text{ball})}(\omega)} \right) \left\{ \frac{\sin(k_F d_{\alpha,\beta})}{\sqrt{\Delta^2 - \omega^2}} \begin{bmatrix} -\omega & \Delta \\ \Delta & -\omega \end{bmatrix} + \cos(k_F d_{\alpha,\beta}) \begin{bmatrix} -1 & 0 \\ 0 & 1 \end{bmatrix} \right\}, \quad (7)$$

where ρ_S is the normal state density of states of the superconductor, $d_{\alpha,\beta}$ the distance between the sites α and β , and $\xi_{\text{BCS}}^{(\text{ball})}(\omega) = \hbar v_F/\sqrt{\Delta^2 - \omega^2}$ the BCS coherence length at a finite energy. The information about propagation in the superconductor in the non local Josephson effect is contained in $f_{\alpha,\beta}(\omega) \equiv g_{\alpha,\beta}^{1,2}(\omega)$, where "1" and "2" refer to the electron and hole Nambu labels respectively. The statistical fluctuations of the Josephson current involve $\overline{(f_{\alpha,\beta}(\omega))^2}$, where the overline is an average over disorder and over the different conduction channels. We have^{32,33}

$$\overline{(f_{\alpha,\beta}(\omega))^2} = \frac{\pi\rho_S}{k_F^2 l_d d_{\alpha,\beta}} \frac{\Delta^2}{\Delta^2 - \omega^2} \exp \left(-\frac{d_{\alpha,\beta}}{\xi_{\text{BCS}}(\omega)} \right), \quad (8)$$

where $\xi_{\text{BCS}}(\omega)$ is the diffusive limit superconducting coherence length.

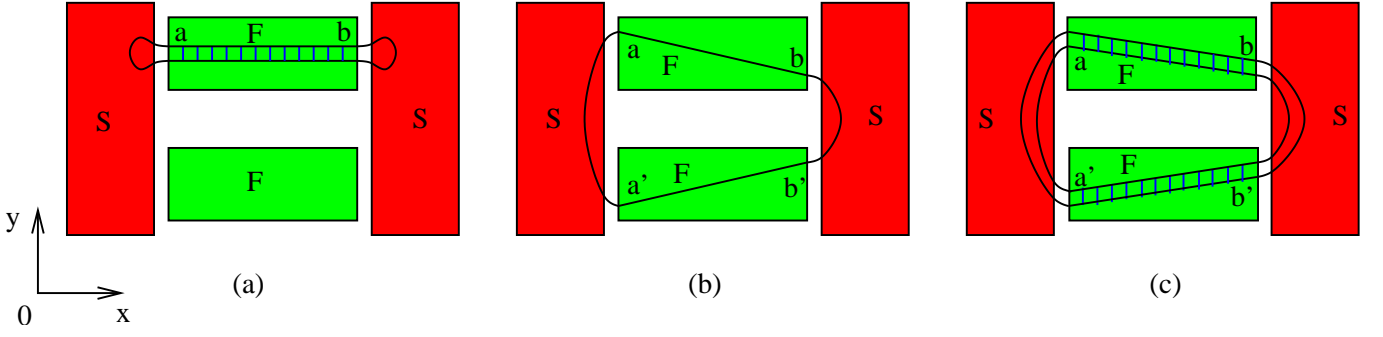


FIG. 3: (Color online.) Schematic representation of the lowest order diagrams for the “local” supercurrent (a), the “non local” supercurrent (b), and the statistical fluctuations of the “non local” supercurrent (c). We represent schematically the ladder diagrams for the diffuson. The rungs of the ladders correspond to a disorder scattering.

C. Supercurrent

The fully dressed Green’s functions $\hat{G}_{i,j}(\omega)$ are obtained from the Dyson equation $\hat{G}(\omega) = \hat{g}(\omega) + \hat{g}(\omega) \otimes \hat{\Sigma} \otimes \hat{G}(\omega)$, where \otimes corresponds to a summation over all the sites in the tunnel Hamiltonian (4). The self-energy is provided by the couplings of the tunnel Hamiltonian, that, in the Nambu representation, take the form

$$\hat{t}_{a,\alpha} = \begin{bmatrix} t_a \exp(i\varphi/4) & 0 \\ 0 & -t_a \exp(-i\varphi/4) \end{bmatrix}, \quad (9)$$

where φ is the phase difference between the two superconductors and t_a is a real number. The phase does not evolve in time since we restrict here to the dc-Josephson effect. The second order diagrams on Fig. 3 contributing the supercurrent acquire a phase $\exp(\pm i\varphi)$, giving rise to a supercurrent proportional to $\sin \varphi$. The equilibrium supercurrent through electrode “a” is given by

$$I_S = \frac{e}{h} \int_0^{+\infty} \text{Tr} \left\{ \hat{\sigma}^z \left[\hat{t}_{\alpha,a} \left(\hat{G}_{a,\alpha}^A(\omega) - \hat{G}_{a,\alpha}^R(\omega) \right) - \hat{t}_{a,\alpha} \left(\hat{G}_{\alpha,a}^A(\omega) - \hat{G}_{\alpha,a}^R(\omega) \right) \right] \right\} d\omega + (h_{ex} \rightarrow -h_{ex}), \quad (10)$$

where the trace is a summation over the Nambu labels and the different conduction channels. The term $(h_{ex} \rightarrow -h_{ex})$ corresponds to the contribution in the sector $S_z = -1/2$. Eq. (10) can be demonstrated from the expression of the current in terms of the Keldysh Green’s function^{34,35}. The transparency of a single junction in the normal state is proportional to $(t/\epsilon_F)^2$, where ϵ_F is the Fermi energy. We suppose here that $t \ll \epsilon_F$, so that the supercurrent is expanded to order $t^4 \rho_S^2 \rho_F^2$. The tunnel supercurrent coupling coherently the two ferromagnets is provided by the emission of a correlated pair of electrons from the left superconductor by Andreev reflection, followed by the absorption of the correlated pair by an Andreev reflection at the right superconductor. These two Andreev reflections can be “local” or “non local” in the sense that the incoming electron and outgoing hole can propagate in identical or in different electrodes.

The local term $I_S^{(\text{loc})}$ in the supercurrent involves a diagram with propagation in a single ferromagnet (see Fig. 3-(a)), such that the incoming electron and the Andreev reflected hole are scattered by the same sequence of impurities:

$$I_S^{(\text{loc})} = 4\pi \frac{e}{h} \Delta |t_{a,\alpha}|^2 |t_{b,\beta}|^2 (\pi \rho_S)^2 \sin \varphi \text{Re} \left\{ \overline{\sum_{a,b} g_{a,b}^{\uparrow,1,A}(\Delta) g_{b,a}^{\uparrow,2,A}(\Delta)} \right\} + (h_{ex} \rightarrow -h_{ex}), \quad (11)$$

where the overline is a disorder averaging, and where the sites a and b belongs to the left and right interfaces respectively (see Fig. 3a). To obtain Eq. (11), we start from Eq. (10), use several times the Dyson equation, and replace the Green’s functions of the isolated ferromagnets and superconductors by Eqs. (5), (6) and (7). The integral over energy is then calculated by contour integration. The poles of the products of the anomalous Green’s functions are at $\omega = \Delta$, so that the ferromagnet Green’s functions are evaluated at $\omega = \Delta$ in Eq. (11).

The spectral “non local” supercurrent involves a diagram with propagation in both ferromagnets (see Fig. 3-(b)):

$$I_S^{(\text{nonloc})}(\omega) = 2\pi \frac{e}{h} \Delta |t_{a,\alpha}|^2 |t_{b,\beta}|^2 \sin \varphi \text{Re} \left[\sum_{a,b,a',b'} \{ f_{\alpha,\beta}(\omega) f_{\alpha',\beta'}(\omega) \right]$$

$$\begin{aligned} & \times \left[g_{a,b}^{\uparrow,1,A}(\omega) g_{b',a'}^{\uparrow,2,A}(\omega) + g_{a,b}^{\uparrow,2,A}(\omega) g_{b',a'}^{\uparrow,1,A}(\omega) \right] \} \} \\ & + (h_{ex} \rightarrow -h_{ex}), \end{aligned} \quad (12)$$

$$(13)$$

where the sites a, b, a' and b' belong to different interfaces (see Fig. 3-(b)). The variance of the non local supercurrent is obtained by integrating the square of the spectral supercurrent given by Eq. (13) over energy and averaging over disorder:

$$\overline{(I_S^{(\text{nonloc})})^2} = \int d\omega \overline{(I_S^{(\text{nonloc})}(\omega))^2}. \quad (14)$$

III. EVALUATION OF THE AVERAGE LOCAL SUPERCURRENT

The average over disorder of the product $\overline{g_{a,b}^{\uparrow,1,A} g_{b,a}^{\uparrow,2,A}}$ in Eq. (11), is evaluated in the ladder approximation in the Appendix. We find³¹

$$\overline{g_{a,b}^{\uparrow,1,A} g_{b,a}^{\uparrow,2,A}} = -\frac{(\pi\rho_F)^2}{k_F^2 l_d d_{a,b}} \exp(iK_h d_{a,b}) \exp(-d_{a,b}/\xi_h), \quad (15)$$

where $d_{a,b}$ is the distance between the sites ‘‘a’’ and ‘‘b’’. The decay length of the supercurrent of a single SFS junction in the diffusive limit is given by³¹

$$\frac{1}{\xi_h} = \sqrt{\frac{3}{2l_d}} \sqrt{\sqrt{\left(\frac{2}{l_\varphi^{(\text{ball})}}\right)^2 + (\Delta k)^2} + \frac{2}{l_\varphi^{(\text{ball})}}}, \quad (16)$$

where the exchange field enters through $\Delta k = k_F^\uparrow - k_F^\downarrow$, equal to the difference between the spin-up and spin-down Fermi wave vectors, with $\Delta k = 2h/v_F$. The wave vector of the supercurrent oscillations^{21,22,23,24,25,26,27,28,29,30} is given by

$$K_h = \sqrt{\frac{3}{2l_d}} \sqrt{\sqrt{\left(\frac{2}{l_\varphi^{(\text{ball})}}\right)^2 + (\Delta k)^2} - \frac{2}{l_\varphi^{(\text{ball})}}}, \quad (17)$$

where l_d is the elastic mean free path. Due to the exchange field, the decay length ξ_h given by Eq. (16) is smaller than the phase coherence length

$$l_\varphi = \sqrt{\frac{l_d l_\varphi^{(\text{ball})}}{3}}. \quad (18)$$

Eqs. (16) and (17) follow from the identity

$$\frac{1}{\xi_h} + iK_h = \sqrt{\frac{3}{l_d} \left(\frac{2}{l_\varphi^{(\text{ball})}} + i\Delta k \right)}, \quad (19)$$

demonstrated in the Appendix.

After summing over all pairs of sites (a, b) at the interface, as detailed in the Appendix, we obtain

$$\begin{aligned} I_S^{(\text{loc})} &= 8\pi \frac{e}{h} N_{\text{ch}} \Delta |t_{a,\alpha}|^2 |t_{b,\beta}|^2 \frac{\pi^4 \rho_S^2 \rho_F^2}{k_F^2 l_d a_0^2} \frac{1}{\sqrt{(1/\xi_h)^2 + K_h^2}} \\ &\exp(-R/\xi_h) \cos(K_h R - \theta), \end{aligned} \quad (20)$$

with $\tan \theta = K_h/\xi_h$. The local supercurrent is then proportional to the number of channels N_{ch} at a single interface, N_{ch} being itself proportional to the area of a single junction.

IV. STATISTICAL FLUCTUATIONS OF THE NON LOCAL SUPERCURRENT

The average of the non local supercurrent vanishes because of disorder averaging in the diffusive system⁹, or because of averaging over the Fermi oscillations in the ballistic system. The disorder average of the square of the non local supercurrent $(I_S^{(\text{nonloc})})^2$ involves the diagrams on Fig. 3-(c), the average over disorder of which does not decay exponentially over the elastic mean free path l_d .

The non local supercurrent (13) can be recast in the form

$$I_S^{(\text{nonloc})} = \mathcal{A} \sum_{a,b,a',b'} \sum_{\sigma,\tau} \left(X_{a,b,a',b'}^{(\sigma,\tau),A} + X_{a,b,a',b'}^{(\sigma,\tau),R} \right), \quad (21)$$

where $\mathcal{A} = \pi(e/h)\Delta|t_{a,\alpha}|^2|t_{b,\beta}|^2$, and $X_{a,b,a',b'}^{(\sigma,\tau)} = f_{\alpha,\beta}f_{\alpha',\beta'}g_{a,b}^{(\sigma,\tau)}g_{b',a'}^{(\sigma,\bar{\tau})}$, and where $\sigma = \uparrow, \downarrow$ is the projection of the spin along the z axis, and $\tau = 1, 2$ is the Nambu index. The notation $\bar{\tau}$ in the definition of $X_{a,b,a',b'}^{(\sigma,\tau)}$ corresponds to $\bar{\tau} = 1$ if $\tau = 2$, and $\bar{\tau} = 2$ if $\tau = 1$. We deduce from Eq. (21)

$$\overline{(I_S^{(\text{nonloc})})^2} = 2\mathcal{A}^2 \sum_{a,b,a',b'} \sum_{\sigma,\tau} \sum_{\sigma',\tau'} \text{Re} \left[X_{a,b,a',b'}^{(\sigma,\tau),A} X_{a,b,a',b'}^{(\sigma',\tau'),A} + X_{a,b,a',b'}^{(\sigma,\tau),A} X_{a,b,a',b'}^{(\sigma',\tau'),R} \right], \quad (22)$$

corresponding to the diagrams on Fig. 3-(c). The disorder averages in each electrode are then carried out, following the Appendix. Factoring out the propagators in the superconductor³⁶, and carrying out the summation over the conduction channels, leads to

$$\begin{aligned} \overline{(I_S^{(\text{nonloc})})^2} &= 4\pi^2(e/h)^2\Delta^2|t_{a,\alpha}|^4|t_{b,\beta}|^4 N_{\text{ch}}^2 \overline{f_{\alpha,\beta}^2} \overline{f_{\alpha',\beta'}^2} \left(\frac{(\pi\rho_S)^2 l_\varphi}{(k_F a_0)^2 l_d} \right)^2 \\ &\times \left\{ \exp\left(-\frac{2R}{l_\varphi}\right) + \frac{1}{\sqrt{1 + (l_\varphi(k^\dagger - k^\downarrow))^2}} \exp\left(-\frac{2R}{\xi_h}\right) \right\} \sin^2 \varphi, \end{aligned} \quad (23)$$

where we discarded the terms decaying exponentially over the Fermi wave-length. The product $\overline{f_{\alpha,\beta}^2} \overline{(f'_{\alpha,\beta})^2}$ is proportional to $1/D^2$, with D^2 of order $N_{\text{ch}} a_0^2 (D/r)^2$, so that $\overline{(I_S^{(\text{nonloc})})^2}$ scales like N_{ch} (see Fig. 2 for the notations D and r). The variance of the supercurrent given by Eq. (23) involves a ‘‘long range’’ contribution decaying over l_φ , and a short range contribution decaying over ξ_h . The former propagates over a much larger distance than the latter. Both contributions are identical for normal metals, but the long range contribution dominates for ferromagnets with $\xi_h \lesssim R \lesssim l_\varphi$.

V. CONCLUSIONS

To conclude, we have investigated the possibility of coupling coherently two superconductors by two spatially separated ferromagnets. The statistical fluctuations of the Josephson current are proportional to the square root of the surface of the junctions. The fluctuating part of the Josephson current is ‘‘long range’’ in the sense that it does not decay over the exchange length ξ_h , but decays over the phase coherence length l_φ . We predict a Josephson current mediated by fluctuations if the length of the ferromagnets is larger than ξ_h and smaller than l_φ . The supercurrent is expected to fluctuate as a function of the relative spin orientation of the ferromagnets. This effect can be used as a test of the phase coherence of crossed Andreev reflection, without the competition between the crossed Andreev reflection and elastic cotunneling channels^{4,7} since the Josephson effect probes solely the anomalous propagator in the superconductor.

Another proposal has been made recently to probe a long range Josephson effect in ferromagnets with non collinear magnetizations in a single SFS junction, generating triplet correlations^{37,38} that can also propagate up to l_φ . This effect is not equivalent to the one considered here since it involves propagation in a single electrode. The fluctuations of the Josephson current discussed here are also not equivalent to universal conductance fluctuations³⁹ since the root mean square of the supercurrent distribution is proportional to the square root of the junction area.

Acknowledgments

The author acknowledges fruitful discussions with D. Feinberg, and thanks H. Courtois for useful comments on the manuscript.

APPENDIX A: DETAILS OF DISORDER AVERAGING

1. Elastic scattering time

The Green's function $\hat{G}^{(0)}(\mathbf{k}, \omega)$ of a disordered isolated ferromagnet, diagonal in the Nambu representation, is given by $\hat{G}^{(0)}(\mathbf{k}, \omega) = \hat{g}(\mathbf{k}, \omega) \left[\hat{I} + \hat{\Sigma}_v \hat{G}^{(0)}(\mathbf{k}, \omega) \right]$, where $\hat{g}(\mathbf{k}, \omega)$ is the Green's function of a ballistic isolated ferromagnet, and

$$\hat{\Sigma}_v = nv^2 \int \frac{d\mathbf{k}'}{(2\pi)^3} \hat{g}(\mathbf{k}', \omega), \quad (\text{A1})$$

is the disorder self-energy, where n is the concentration of impurities. Evaluating the integral in Eq. (A1) by contour integration leads to

$$\hat{G}^{(0),\uparrow,1,A}(\mathbf{k}, \omega) = \frac{1}{\omega - h - \xi_k - i/\tau_{1,1}} \quad (\text{A2})$$

$$\hat{G}^{(0),\uparrow,2,A}(\mathbf{k}, \omega) = \frac{1}{\omega - h + \xi_k - i/\tau_{2,2}}, \quad (\text{A3})$$

with

$$\tau_{1,1} = \frac{\tau}{1 + \omega/2\epsilon_F - h/2\epsilon_F} \quad (\text{A4})$$

$$\tau_{2,2} = \frac{\tau}{1 - \omega/2\epsilon_F + h/2\epsilon_F}, \quad (\text{A5})$$

with $\tau = 4\pi\epsilon_F/(k_F^3 v^2)$ the elastic scattering time with $h = \omega = 0$.

2. Disorder averaging of the supercurrent

The supercurrent involves the disorder average $\overline{g_{a,b}^{\uparrow,1,A}(\omega) g_{b,a}^{\uparrow,2,A}(\omega)}$, evaluated in Fourier space in the ladder approximation³³. Using contour integration, we find

$$\int \frac{d\mathbf{k}}{(2\pi)^3} \hat{G}^{\uparrow,1,A}(\mathbf{k}, \omega) \hat{G}^{\uparrow,2,A}(\mathbf{k} + \mathbf{q}, \omega) \simeq -1 + i\tau(\omega - h + iv_F/l_\varphi^{(\text{ball})}) + \frac{q^2 \tau^2 \epsilon_F^2}{3k_F^2}. \quad (\text{A6})$$

After the summing the ladder diagrams, the poles are found at wave-vector

$$q^{(\text{diff})} = \sqrt{\frac{6}{l_d} \left(\frac{1}{l_\varphi^{(\text{ball})}} - \frac{ih}{v_F} + \frac{i}{\xi^{(\text{ball})}} \right)}, \quad (\text{A7})$$

where we replaced ω by Δ , as obtained in the energy integration of the local supercurrent [see Eq. (11)]. Eq. (A7) leads directly to Eq. (19) if one assumes the ballistic superconducting coherence length $\xi^{(\text{ball})}$ of the order of $1 \mu\text{m}$ to be large compared to the ballistic exchange length v_F/h and to the ferromagnet ballistic phase coherence length $l_\varphi^{(\text{ball})}$. The geometrical prefactor $(\pi\rho_F)^2/k_F^2 l_e d_{a,b}$ is then obtained by evaluating the residue in the integral over \mathbf{q} .

3. Summation over the conduction channels

The supercurrent given by Eq. (11) involves a summation over the conduction channels. This summation is evaluated through

$$\begin{aligned} \sum_{a,b} \frac{a_0}{d_{a,b}} \exp \left[- \left(\frac{1}{\xi} - iK_h \right) d_{a,b} \right] &\simeq N_{\text{ch}} \int \frac{2\pi y dy}{a_0 \sqrt{R^2 + y^2}} \exp \left[- \left(\frac{1}{\xi} - iK_h \right) \sqrt{R^2 + y^2} \right] \\ &= N_{\text{ch}} \frac{\xi/a_0}{1 - iK_h \xi} \exp \left[- \left(\frac{1}{\xi} - iK_h \right) R \right], \end{aligned} \quad (\text{A8})$$

where $d_{a,b} = \sqrt{R^2 + y^2}$ is the distance between the sites a and b .

4. Disorder averaging from real space Green's functions

The product of the ballistic Green's functions $g_{a,b}^{\uparrow,1,A}(\omega)g_{b,a}^{\uparrow,2,A}(\omega)$ is proportional to $\exp[-q^{(\text{ball})}d_{a,b}]$, with $q^{(\text{ball})} = i\Delta k + 2i\omega/v_F + 2/l_{\varphi}^{(\text{ball})}$. The wave-vector $q^{(\text{diff})}$ given by Eq. (A7) is related to $q^{(\text{ball})}$ according to

$$q^{(\text{diff})} = \sqrt{\frac{3q^{(\text{ball})}}{l_d}}. \quad (\text{A9})$$

- ¹ N. K. Allsopp, V. C. Hui, C. J. Lambert and S. J. Robinson, J. Phys.: Condens. Matter **6**, 10475 (1994).
- ² C.J. Lambert and R. Raimondi, J. Phys.: Condens. Matter **10**, 901 (1998).
- ³ F.J. Jedema, B.J. van Wees, B.H. Hoving, A.T. Filip and T.M. Klapwijk, Phys. Rev. B **60**, 16549 (1999); B. J. van Wees et al. , "Mesoscopic Electron Transport" ed. L. Sohn, L. Kouwenhoven and G. Schön, NATO ASI Series , vol 345 (Kluwer Academic, Dordrecht, 1996).
- ⁴ G. Falci, D. Feinberg, and F.W.J. Hekking, Europhys. Lett. **54**, 255 (2001).
- ⁵ E. Prada and F. Sols, Eur. Phys. J. B **40**, 379 (2004).
- ⁶ R. Mélin and D. Feinberg, Eur. Phys. J. B **26**, 101 (2002).
- ⁷ R. Mélin and D. Feinberg, Phys. Rev. B **70**, 174509 (2004).
- ⁸ R. Mélin, J. Phys.: Condens. Matter **13**, 6445 (2001).
- ⁹ R. Mélin and S. Peysson, Rev. B **68**, 174515 (2003).
- ¹⁰ R. Mélin, H. Jirari and S. Peysson, J. Phys.: Condens. Matter **15**, 5591 (2003).
- ¹¹ G. Deutscher and D. Feinberg, App. Phys. Lett. **76**, 487 (2000).
- ¹² D. Sanchez, R. Lopez, P. Samuelsson and M. Buttiker, Phys. Rev. B **68**, 214501 (2003).
- ¹³ T. Yamashita, S. Takahashi and S. Maekawa, Phys. Rev. B **68** 174504 (2003).
- ¹⁴ N.M. Chtchelkatchev, I.S. Burmistrov, Phys. Rev. B **68**, 140501 (2003).
- ¹⁵ D. Feinberg, Eur. Phys. J. B **36**, 419 (2003).
- ¹⁶ C.J. Lambert, J. Koltai, and J. Cserti, in *Towards the controllable quantum states (Mesoscopic superconductivity and spintronics)*, p. 119, Eds H. Takayanagi and J. Nitta, World Scientific (2003).
- ¹⁷ F. Taddei and R. Fazio, Phys. Rev. B **65**, 134522 (2002).
- ¹⁸ G. Bignon, M. Houzet, F. Pistolesi, and F. W. J. Hekking, Europhys. Lett. **67**, 110 (2004).
- ¹⁹ D. Beckmann, H. B. Weber, and H. v. Löhneysen Phys. Rev. Lett. **93**, 197003 (2004).
- ²⁰ S. Russo, M. Kroug, T. M. Klapwijk, and A. F. Morpurgo, cond-mat/0501564.
- ²¹ A.I. Buzdin, L.N. Bulaevskii, and S.V. Panyukov, Pis'ma Zh. Eksp. Teor. Fiz. **35**, 147 (1982) [JETP Lett. **35**, 178 (1982)].
- ²² Z. Radović, L. Dobrosavljević-Grujić, and B. B. Vujičić, Phys. Rev. B **63**, 214512 (2001).
- ²³ T.T. Heikkilä, F.K. Wilhelm, and G. Schön, Eurphys. Lett. **51**, 434 (2000).
- ²⁴ A.A. Golubov, M. Yu. Kupriyanov, and Ya. V. Fominov, JETP Letters **75**, 588 (2002); **76**, 231 (2002).
- ²⁵ A. I. Buzdin, L. N. Bulaevski, and S. V. Panyukov Pis'ma Zh. Eksp. Teor. Fiz. **35**, 147 (1982) [JETP Lett. **35**, 178 (1982)]; A. I. Buzdin and M. Yu. Kupriyanov Pis'ma Zh. Eksp. Teor. Fiz. **52**, 1089 (1990) [JETP Lett. **52**, 487 (1990)]; A. Buzdin, B. Bujicic, and M. Yu. Kupriyanov, Zh. Eksp. Teor. Fiz. **101**, 231 (1992) [Sov. Phys. JETP **74**, 124 (1992)].
- ²⁶ V.V. Ryazanov, V.A. Oboznov, A.Y. Rusanov, A.V. Veretennikov, A.A. Golubov and J. Aarts, Phys. Rev. Lett. **86**, 2427 (2001).
- ²⁷ V.V. Ryazanov, V.A. Oboznov, A.V. Veretennikov, and A.Y. Rusano, Phys. Rev. B **65**, 020501 (2001).
- ²⁸ T. Kontos, M. Aprili, J. Lesueur, F. Genêt, B. Stephanidis, and R. Boursier, Phys. Rev. Lett. **89**, 137007 (2002).
- ²⁹ W. Guichard, M. Aprili, O. Bourgeois, T. Kontos, J. Lesueur, and P. Gandit, Phys. Rev. Lett. **90**, 167001 (2003).
- ³⁰ H. Sellier, C. Baraduc, F. Lefloch, and R. Calemczuk, Phys. Rev. B **68**, 054531 (2003); Phys. Rev. Lett. **92**, 257005 (2004).
- ³¹ R. Mélin, Europhys. Lett. **69**, 121 (2005).
- ³² D. Feinberg, Eur. Phys. J B **36**, 419 (2003).
- ³³ R. A. Smith and V. Ambegaokar, Phys. Rev. B **45**, 2463 (1992).
- ³⁴ C. Caroli et al., J. Phys. C: Solid St. Phys. **4**, 916 (1971).
- ³⁵ J.C. Cuevas, A. Martín-Rodero and A. Levy Yeyati, Phys. Rev. B **54**, 7366 (1996).
- ³⁶ This assumption is strictly speaking valid only for $D \gg r$ (see Fig. 2). However, Eq. (23) is still valid for $D \sim r$, up to a dimensionless geometrical prefactor.
- ³⁷ F.S. Bergeret, A.F. Volkov and K.B. Efetov, Phys. Rev. Lett. **18**, 4096 (2001).
- ³⁸ A. Kadigrobov, R.I. Shekhter and M. Jonson, Europhys. Lett. **54**, 394 (2001).
- ³⁹ P.A. Lee and A. Douglas Stone, Phys. Rev. Lett. **55**, 1622 (1985).